

Dynamics of D3-D7 Brane Inflation in Throats

Fang Chen^{1*}, Hassan Firouzjahi^{2†}

¹ *Physics Department, McGill University, Montreal, H3A 2T8, Canada.*

² *School of Physics, Institute for Research in Fundamental Sciences (IPM),
P.O.Box 19395-5531, Tehran, Iran*

ABSTRACT: Dynamics of D3-branes in models of warped D3-D7 inflationary set up is studied where perturbative α' correction to the Kähler potential and the nonperturbative corrections to the superpotential are included. It is shown that a dS minimum can be obtained without introducing anti-branes. Some specific configurations of D7-branes embedding were studied. After stabilizing the angular directions, it is shown that the resulting D3-D7 potential of the radial position of the D3-brane is too steep to allow slow-roll inflation. Depending on D7-branes embedding and the stabilized angular directions, the mobile D3-brane can move either towards the tip of the throat or towards the D7-branes.

*fangchen@hep.physics.mcgill.ca

†firouz@ipm.ir

Contents

1. Introduction	1
2. The low energy 4D supergravity	3
2.1 General definitions	3
2.2 Evaluation of the potential	4
2.3 Uplifting	5
3. The conifold	6
4. D3-D7 Brane Inflation Dynamics	9
4.1 Ouyang Embedding	9
4.1.1 Stability of case (a)	11
4.1.2 Stability of case (b)	12
4.2 Kuperstein Embedding	13
5. Conclusion and Discussions	14
A. Uplifting by α' correction	15
B. The Conifold	16
C. The stability analysis	17
C.1 Ouyang embedding	17
C.1.1 Stability of case (a)	18
C.1.2 Stability of case (b)	19
C.2 Kuperstein Embedding	19

1. Introduction

Obtaining metastable de Sitter vacua and inflation within type IIB string theory has been a major focal point of string cosmology in recent years. Compactifications making use of warped throats [1, 2] have provided a self-consistent starting point, but the simplest versions lead to AdS rather than Minkowski or dS minima. The introduction of anti-D3 branes into the throat can uplift the AdS minimum [3], and can allow for brane-antibrane inflation [4].

However the antibranes explicitly break supersymmetry, while the low-energy description of the Kähler moduli and inflaton field is in the language of supergravity. This tension has

motivated the search for other uplifting mechanisms which are not explicitly SUSY-breaking, notably magnetic fluxes on the D7-branes, leading to D-term uplifting [5]. Other examples include ref. [6], in which it is pointed out that the back reaction of D7-branes leads to a correction of the dilaton background that can give uplifting in the presence of D3 branes.

The present work is motivated by the possible interplay between the mechanism of uplifting and the naturalness of brane-antibrane inflation [7, 8] in the warped throat (for an extensive review on brane inflation see [9] and references therein). These two issues are related through the infamous η problem [4]: because the D3-brane modulus (which is also the inflaton) ϕ enters into the Kähler potential K through the combination $R = 2\sigma(1 - c\phi^2/M_p^2)$ (where σ is the Kähler modulus and $c \sim 1$) and all terms in the inflaton potential go like $1/R^p$ with p being a positive power, the inflaton mass is naturally of order $V/M_p^2 = H^2$, and so the inflationary η parameter is $O(1)$. The inflaton mass can be made small only by finely-tuned competing contributions, notably the ϕ dependent corrections to the nonperturbative superpotential [6, 10, 11, 12, 13, 14].

As in [2], we assume that all complex structures are stabilized by turning a variety of background fluxes. The resulting classical superpotential is independent of the Kähler modulus leading to a no-scale potential where the Kähler modulus remains completely undetermined. The no-scale property of the potential can be broken either via non-perturbative corrections to the superpotential as employed in [3], or via perturbative α' correction into the Kähler potential as demonstrated in [15]. In [15] it is shown that the leading corrections are in the form of $K = -2\ln(R^{3/2} + \xi)$ where ξ represents the α'^3 correction to the Kähler potential. Uplifting using this α' correction into the Kähler potential was discussed previously in [16, 17, 18]. We also find that in our D3-D7 setup uplifting can be achieved from the interplay of leading perturbative α' correction and non-perturbative superpotential corrections, without any antibrane. Since the higher order α' correction into the Kähler potential are not known, we work in a large volume limit where only the leading perturbative α' correction into the Kähler potential are trusted. Also we work in the limit where the constant term in the superpotential W_0 to be much larger than in the KKLT [3] proposal, which is a virtue since the KKLT value is unnaturally small.

Having obtained a dS vacuum, we add the D3-brane into the setup. As in [13], we take into account the D3-brane corrections into the non-perturbative superpotential. This results in a potential for the mobile D3 brane in the throat. To study its suitability for inflation, we must minimize the potential with respect to the angular directions in the throat for a given radial position r , resulting in the effective single-field inflaton potential (since $\phi \propto r$). We perform this minimization for two characteristic embeddings of the D7 branes in the throat, the Ouyang and Kuperstein embeddings [19, 20]. In neither case can $V(\phi)$ be made flat enough to give inflation. The problem can be traced to the requirement of large W_0 . The nonperturbative superpotential corrections, which were tuned to cancel the contributions to η coming from W_0 in [14], cannot be made sufficiently large to enable this cancellation when $|W_0| \sim 1$.

We begin in section 2 with the 4D supergravity effective action describing the Kähler

modulus and D3 brane modulus, including the effect of α' corrections in the Kähler potential. Here we give a detailed realization of the uplifting due to such corrections. In section 3 we review the description of the geometry of the conifold to introduce the angular degrees of freedom of the D3-brane in the throat. These angles are minimized at different values, depending on the embedding of the D7 branes and the radial position of the D3 in the throat. In section 4 we determine these angular minima for two representative D7 embeddings which have been discussed in previous literature. For each case we show that the potential for the radial modulus of the D3-brane cannot be tuned to be flat enough for inflation. In the final section 5, we argue that this is a generic feature of large volume compactifications.

2. The low energy 4D supergravity

We start with the 4D effective supergravity for the dynamics of two light fields: T , describing the volume modulus and z^i denoting the position in the extra dimensions of the D3 brane. We suppose the dynamics of these fields to be governed by gaugino condensation on the D7 brane, in the usual KKLT fashion, including the back-reaction of the D3 brane as computed by Baumann et. al. [13].

2.1 General definitions

The Kähler potential, K , and superpotential, W , defining the low-energy 4D supergravity are given by [15]

$$\begin{aligned} K &= -2 \ln(R^{3/2} + \xi) \\ W &= W_0 + A(z) \exp[-bT]. \end{aligned} \tag{2.1}$$

where $T = \sigma + i\tau$ is the complex Kähler modulus, τ is the axion-dilaton field and σ is the volume modulus. More specifically, $\sigma^{1/4}$ measures the size of the CY compactification

$$\sigma \sim \frac{R_{CY}^4}{\alpha'^2}. \tag{2.2}$$

Here R_{CY} represents the average radius of the CY compactification. To trust low energy supergravity formalism, we require $\sigma \gg 1$. We take $\sigma \sim \mathcal{O}(100)$ in our discussions below. Also

$$R = T + \bar{T} - \gamma k(z, \bar{z}) = 2\sigma - \gamma k(z, \bar{z}). \tag{2.3}$$

Here $k(z, \bar{z})$ denotes the Kähler potential for the CY geometry with the Kähler metric $k_{i\bar{j}} = \partial_i \partial_{\bar{j}} k(z, \bar{z})$ and $z^i, i = 1, 2, 3$ represent the position of the mobile D3-brane inside CY compactification. Also $A(z) = A_0 [F(z)]^{1/n}$ where the holomorphic condition $F(z) = 0$ defines the position of the stack of n D7 branes in this geometry. The exponential term in W represents the non-perturbative correction to the superpotential coming from the gaugino condensation on coincident D7-branes and $b = 2\pi/n$. Finally, γ is related to the tension of

the D3-brane and is given by

$$\gamma = \frac{\sigma}{3} \frac{T_3}{M_P^2} \quad (2.4)$$

where $T_3 \sim m_s^4$ is the tension of the D3-brane.

The F-term potential is computed from K and W using the standard formula

$$\begin{aligned} V_F &= e^K \left[K^{\bar{a}b} \overline{D_a W} D_b W - 3|W|^2 \right] \\ &= e^K \left[(K^{\bar{a}b} K_{\bar{a}} K_b - 3)|W|^2 + K^{\bar{a}b} \overline{W}_a W_b + K^{\bar{a}b} W \overline{W}_a K_b + K^{\bar{a}b} \overline{W}_b W K_{\bar{a}} \right], \end{aligned} \quad (2.5)$$

where $D_a W = W_a + K_a W$ and $K^{\bar{a}b}$ denotes the inverse, $K^{\bar{a}b} K_{b\bar{c}} = \delta^{\bar{a}}_{\bar{c}}$, of the Kähler metric on moduli space, $K_{b\bar{c}} = \partial_b \partial_{\bar{c}} K$.

2.2 Evaluation of the potential

We now explicitly evaluate the derivatives appearing in the above definitions, using the given functions K, W . The superpotential derivatives become

$$W_T = -bA \exp(-bT), \quad W_i = A_i \exp(-bT), \quad (2.6)$$

where the superscript i represents the partial derivative with respect to z^i the position of the mobile D3-brane. It is useful to define $\hat{\xi} = \xi R^{-3/2}$ and $\hat{R} = R(1 + \hat{\xi})$ where the Kähler potential is now given by

$$K = -2 \ln(R^{1/2} \hat{R}). \quad (2.7)$$

In this notation, the quantity $\hat{\xi}$ measures the strength of α' correction to the Kähler potential. The consistency of our perturbation requires that $\hat{\xi} \ll 1$.

The Kähler derivatives are given by

$$K_T = -\frac{3}{\hat{R}}, \quad K_i = \frac{3\gamma k_i}{\hat{R}}, \quad (2.8)$$

where here and below $k_i \equiv \partial_i k$ and $k_{\bar{i}} \equiv \partial_{\bar{i}} k$.

The Kähler derivatives of W evaluate to

$$\begin{aligned} D_T W &= -\frac{3W_0}{\hat{R}} - A \exp(-bT) \left(b + \frac{3}{\hat{R}} \right) \\ D_i W &= \frac{3\gamma W_0 k_i}{\hat{R}} + A \exp(-bT) \left(\frac{A_i}{A} + \frac{3\gamma k_i}{\hat{R}} \right). \end{aligned}$$

The Kähler metric is given by

$$K_{\bar{a}b} = \frac{3}{\hat{R}\check{R}} \begin{pmatrix} 1 & -\gamma k_{\bar{j}} \\ -\gamma k_i & \gamma \check{R} k_{i\bar{j}} + \gamma^2 k_i k_{\bar{j}} \end{pmatrix}, \quad (2.9)$$

where

$$\check{R} \equiv \frac{2(1 + \hat{\xi})}{(2 - \hat{\xi})} R. \quad (2.10)$$

After some algebra, the inverse metric is

$$K^{\bar{a}b} = \frac{\hat{R}}{3} \begin{pmatrix} \check{R} + \gamma k^{\bar{i}} k_{\bar{i}} & k^i \\ k^{\bar{j}} & \gamma^{-1} k^{\bar{j}i} \end{pmatrix}, \quad (2.11)$$

where $k^{\bar{i}j}$ is the inverse of $k_{\bar{i}j}$ with $k^{\bar{i}j} k_{\bar{j}l} = \delta_{\bar{l}}^{\bar{i}}$ and $k^i = k_{\bar{j}} k^{\bar{j}i}$.

Calculating the F-term potential from (2.5), one obtains

$$V_F = \frac{1}{3R\hat{R}} \left[|A|^2 e^{-2b\sigma} \left((\check{R} + \gamma k^i k_i) b^2 + 6b \frac{\check{R}}{\hat{R}} \right) + 3bW_0 \frac{\check{R}}{\hat{R}} (Ae^{-bT} + c.c.) \right. \\ \left. - b e^{-2b\sigma} (A k^{\bar{i}} \bar{A}_i + c.c.) + \gamma^{-1} e^{-2b\sigma} k^{\bar{i}j} \bar{A}_i A_j + \frac{9}{\hat{R}^2} (\check{R} - \hat{R}) |W|^2 \right]. \quad (2.12)$$

As in [15, 16] the no-scale property of the four-dimensional supergravity is broken in the presence of ξ . This manifests itself in the last term containing $|W|^2$.

We note that there are two terms in potential (2.12) containing the axion field τ in the form of $W_0(Ae^{-ib\tau} + c.c.)$. Minimizing the potential with respect to τ and noting that $W_0 < 0$, the stable value of axion is given by

$$e^{-ib\tau} = \left(\frac{\bar{A}}{A} \right)^{1/2}. \quad (2.13)$$

As mentioned in [14], plugging this value of the axion field into the potential (2.12), is equivalent to replacing $(Ae^{-ib\tau} + c.c.)$ by $2|A|$, which we consider is the case from now on.

2.3 Uplifting

In this section we study the uplifting and the stabilization in the absence of the mobile D3-brane. For uplifting in this mechanism to be achieved, we need to work in the limit where $|W_0| \sim 1$ which is natural in flux compactification. This is opposite of the KKLT limit where $|W_0| \ll 1$ by tuning.

An analytical understanding of the background is very helpful when we include the D3-brane in next section in search for getting inflation. In the absence of D3-brane, $W_i = k_i = 0$, $R = 2\sigma$ and $A = A_0$. Eliminating the axion field as mentioned before, the F-term potential for σ obtained from (2.12), in the convention $A_0 = 1$, is

$$V_F = \frac{1}{24\sigma^3(1 + \hat{\xi})^2(2 - \hat{\xi})} \left[9W_0^2 \hat{\xi} + 6A_0 W_0 e^{-b\sigma} \left(4b\sigma(1 + \hat{\xi}) + 3\hat{\xi} \right) \right. \\ \left. + A_0^2 e^{-2b\sigma} \left(8b\sigma(3 + b\sigma) + (3 + 4b\sigma)^2 \hat{\xi} + 8b^2 \sigma^2 \hat{\xi}^2 \right) \right]. \quad (2.14)$$

As explained before, the breakdown of the no-scale symmetry manifests itself in the term containing W_0^2 , corresponding to the zeroth order contribution of the superpotential to the potential.

In order to get a better understanding of the uplifting and the Kähler modulus stabilization mechanism, here we expand the potential up to quadratic order in terms of $\hat{\xi} = \xi/(2\sigma)^{3/2}$

$$V_F \simeq \frac{bW_0}{2\sigma^2} e^{-b\sigma} + \frac{3W_0^2 \xi}{2^{11/2} \sigma^{9/2}} - \frac{9W_0^2 \xi^2}{256 \sigma^6}. \quad (2.15)$$

We assume that W_0 is large enough, possibly $\mathcal{O}(10)$, such that terms containing $e^{-2b\sigma}$ are negligible. The details of the conditions for uplifting and stabilization of the Kähler modulus is relegated to the **Appendix A**. In the limit of small $\hat{\xi}$, we find the following approximation relations

$$b\sigma \simeq 3 \quad , \quad |W_0| \xi b^{3/2} \simeq 6. \quad (2.16)$$

Using the relation $b = 2\pi/n$, we find that $\sigma \simeq n/2$ and $W_0 \sim \hat{\xi}^{-1}$. For uplifting to work in this mechanism we need to start with large enough $|W_0|$ as mentioned before. Also to obtain a large enough compactification, we should start with a large enough number of wrapped D7-branes.

Here we provide some examples where potential (2.14) can be stabilized to a dS vacuum. For the first example, suppose $A_0 = 1$, $W_0 = -8$ and $n = 157$, corresponding to $b = 0.04$. Then there are dS minima for the range $104 \lesssim \xi \lesssim 109$, with $60 \lesssim \sigma_{min} \lesssim 68$. If required, one can tune ξ to obtain a Minkowski vacuum. One also finds that $\hat{\xi} < 0.08$ so one may consider the effect of α' corrections perturbatively. To get a larger value of Kähler modulus, one can increase the number of D7-branes, as mentioned above. Choosing $b = 0.02$, corresponding to $n = 314$ and with $A_0 = 1$ and $W_0 = -8$ as above, the dS vacua exist for $292 \lesssim \xi \lesssim 311$, corresponding to $120 \lesssim \sigma_{min} \lesssim 145$. Like before, $\hat{\xi} < 0.08$. A plot of the potential for $\xi = 300$ is given in **Fig 1**. We also note that the approximate relations given in Eq. (2.16) are satisfied to a reasonable accuracy in these two examples.

3. The conifold

We work in the background where the ten-dimensional metric is in the form of warped geometry

$$ds^2 = h(r)^{-1/2} ds_4^2 + h(r)^{1/2} ds_6^2, \quad (3.1)$$

where $h(r)$ is the warp factor.

To incorporate the position of D3-brane in the potential, we need to know $k(z, \bar{z})$, the Kähler potential of the CY space. For applications to the throat we specialize to the conifold defined by

$$\sum_{m=1}^4 z_m^2 = 0 \quad (3.2)$$

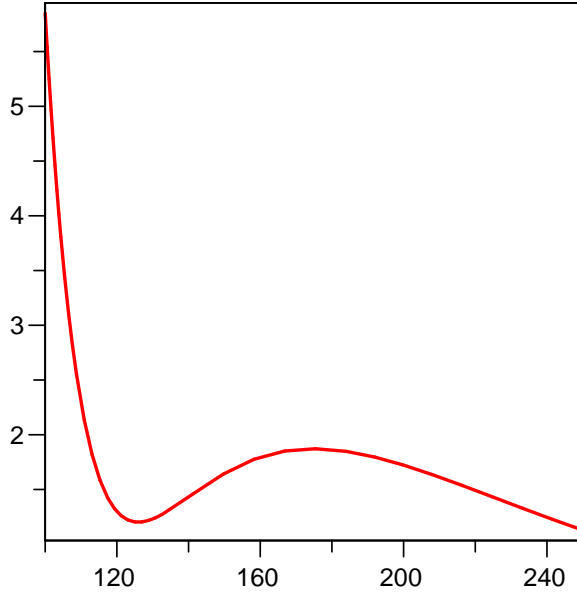


Figure 1: In this figure, V_F versus σ is plotted for $A_0 = 1, W_0 = -8, n = 314$ with $\xi = 300$. The vertical line is in units of 10^{-8} .

where $\{z_m, m = 1, 2, 3, 4\}$ are complex coordinates. The metric of the cone can also be written as

$$ds_6^2 = dr^2 + r^2 ds_{T^{11}}^2 \quad (3.3)$$

where $ds_{T^{11}}^2$ is the metric of the base, T^{11} , which is a five-dimensional Einstein manifold given by

$$ds_{T^{11}}^2 = \left[\frac{1}{9} \left(d\psi + \sum_{k=1,2} \cos \theta_k d\phi_k \right)^2 + \frac{1}{6} \sum_{k=1}^2 \left(d\theta_k^2 + \sin^2 \theta_k d\phi_k^2 \right) \right] \quad (3.4)$$

where $\theta_i \in [0, \pi], \phi_i \in [0, 2\pi]$ and $\psi \in [0, 4\pi]$.

The metric of the cone is given by the Kähler potential

$$k = \left(\sum_{m=1}^4 |z_m|^2 \right)^{2/3} = r^2. \quad (3.5)$$

Eq. (3.2) describes a singular cone. To remove the singularity at $r = 0$, as in Klebanov-Strassler (KS) [1], one can work with the deformed conifold where the sum in Eq. (3.2) is equal to ϵ^2 . Here ϵ^2 is a parameter of dimension length to the power of 3 which measures the deformation of the cone at the tip and its value is given by the value of warp factor at the tip. In this work, we assume that the D3-brane is located far away from the tip such that

our analysis is not sensitive to the details of the deformation. Furthermore, for simplicity we also assume that the infra-red geometry of the cone is cut-off at $r = r_0$.

In the construction of KS, the warp factor is produced by the background F_3 and H_3 fluxes turned on inside different three-cycles present inside the cone. To a good approximation, one can take the warp geometry in the form of

$$h(r) = \frac{R^4}{r^4}, \quad (3.6)$$

where R measures the curvature radius of the AdS geometry given by

$$R^4 = \frac{27}{4}\pi g_s N \alpha'^2. \quad (3.7)$$

Here $N = MK$ is the background flux with K and M being the numbers of H_3 and F_3 fluxes respectively. Furthermore, the value of warp factor at the tip, $r = r_0$, denoted by h_0 , is given by

$$h_0 \equiv h^{-1/4}(r_0) = \frac{r_0}{R} = e^{-2\pi K/3g_s M}. \quad (3.8)$$

We are interested in the radial motion of the mobile D3-brane inside the throat. In the absence of interaction between D3 and D7-branes, the D3-brane moves freely in the AdS-type background above. However, once the interaction between D3 and D7-branes are taken into account, D3-brane will not be free anymore. We would like to study the motion of the D3-brane once the perturbative Kähler corrections and nonperturbative correction to superpotential are included. This problem was previously studied in [6, 14, 21, 22, 23] where the background is in the limit of KKLT where $|W_0| \ll 1$ by tuning and the perturbative corrections to Kähler potential is neglected, i.e. $\xi = 0$.

In [6] the motion of D3-brane in Ouyang embedding [19] was studied. In [14] this was generalized to other embeddings such as Kuperstein embedding [20]. In this work we formulate the potential for the D3-brane for generic embeddings and specialize to the above two embeddings.

From the Kähler potential of the cone given as in Eq. (3.5), one obtains

$$k_{i\bar{j}} = \frac{2}{3r} \left[\delta_{i\bar{j}} + \frac{z_i \bar{z}_j}{|z_4|^2} - \frac{1}{3r^3} \left(z_i \bar{z}_j + z_j \bar{z}_i - z_i z_j \frac{\bar{z}_4}{z_4} - \bar{z}_i \bar{z}_j \frac{z_4}{\bar{z}_4} \right) \right] \quad (3.9)$$

where $i = 1, 2, 3$ and we eliminated z_4 in terms of z_1, z_2 and z_3 using the definition of cone Eq. (3.2). For the inverse metric, denoted by $k_{(z)}^{\bar{i}j}$, we obtain

$$k_{(z)}^{\bar{i}j} = \frac{3r}{2} \left[\delta^{\bar{i}j} + \frac{\bar{z}_i z_j}{2r^3} - \frac{\bar{z}_j z_i}{r^3} \right]. \quad (3.10)$$

Alternatively, one can work with the w -coordinate which is defined by the following linear relation to the z -coordinate

$$\begin{pmatrix} w_1 & w_2 \\ w_3 & w_4 \end{pmatrix} = \frac{1}{\sqrt{2}} \begin{pmatrix} z_1 + iz_2 & z_1 - iz_2 \\ z_3 + iz_4 & -z_3 + iz_4 \end{pmatrix}. \quad (3.11)$$

For a review of the construction of the cone in z and w coordinates see **Appendix B**.

The Kähler metric in w -coordinate is now given by

$$k_{i\bar{j}} = \frac{2}{3r} \left[\delta_{i\bar{j}} + \frac{c_i^k c_{\bar{j}}^s}{|w_3|^2} w_k \bar{w}_s - \frac{1}{3r^3} (\bar{w}_i w_j + \frac{\bar{w}_4}{w_3} c_i^k w_k w_j + \frac{w_4}{\bar{w}_3} c_{\bar{j}}^s \bar{w}_s \bar{w}_i + \frac{|w_4|^2}{|w_3|^2} c_j^s c_i^k \bar{w}_s w_k) \right] \quad (3.12)$$

where the non-zero components of the matrix c_j^i given as in [14] are $c_2^1 = c_1^2 = 1$ and $c_3^4 = -1$. Calculating the inverse metric, denoted by $k_{(w)}^{\bar{i}j}$, one obtains

$$k_{(w)}^{\bar{i}j} = \frac{3r}{2} \left[\delta^{\bar{i}j} + \frac{\bar{w}_i w_j}{2r^3} - \frac{c_i^{i'} c_j^{j'} w_{i'} \bar{w}_{j'}}{r^3} \right]. \quad (3.13)$$

One can also check that the following relations hold which would be helpful later on in calculating the potential

$$k^i \equiv k_{\bar{j}} k_{(z)}^{\bar{j}i} = \frac{3}{2} z^i, \quad k^i k_i = k = r^2, \quad (3.14)$$

with a similar relations also for w -coordinate.

4. D3-D7 Brane Inflation Dynamics

In this section we calculate the potential between D3 and D7 branes in the throat and see whether or not a period of slow-roll inflation can be achieved (for an update on D3-D7 inflation [24], see [25]). The D3-D7 potential is a function of the radial as well as the azimuthal positions of the D3-brane. After finding the stable angular directions of the mobile brane, the potential is studied as a function of the radial position of the D3-brane which plays the role of the inflation field.

To calculate the F-term potential we need to specify the form of the holomorphic function $F(z)$, determining the embedding of the stack of D7-branes in this configuration. As explained before, we shall specialize to Kuperstein and Ouyang embeddings which define two characteristic classes of embeddings.

4.1 Ouyang Embedding

The Ouyang embedding is defined in the w -coordinate via

$$\begin{aligned} F(w) &= 1 - \frac{w_1}{\mu} \\ &= 1 - \left(\frac{r}{r_\mu}\right)^{3/2} e^{\frac{i}{2}(\psi - \phi_1 - \phi_2)} \sin \frac{\theta_1}{2} \sin \frac{\theta_2}{2}. \end{aligned} \quad (4.1)$$

Here μ is a parameter of dimension length to the power of 3/2. One can define the length parameter r_μ via $r_\mu = \mu^{2/3}$. Schematically, r_μ represent the distance of the D7-brane from the

throat. Using the embedding Eq. (4.1), the contribution of the D3-brane to the superpotential is

$$A(w_1) = A_0 \left(1 - \frac{w_1}{\mu}\right)^{1/n}. \quad (4.2)$$

Including the contribution of the D3-brane into superpotential, the F-term potential calculated from Eq. (2.12) is now given by

$$V_F = \frac{\mathcal{F}^{1/n}}{3R\hat{R}} \left[a_1 + a_2 \left(2 - \frac{w_1 + \bar{w}_1}{\mu}\right) \mathcal{F}^{-1} + a_3 \mathcal{F}^{-1/2n} + a_4 k_w^{\bar{1}1} \mathcal{F}^{-1} \right] + \frac{a_5}{3R\hat{R}} \quad (4.3)$$

where

$$\mathcal{F} \equiv |F|^2 = \left(1 - \frac{w_1 + \bar{w}_1}{\mu} + \frac{|w_1|^2}{\mu^2}\right) \quad (4.4)$$

and a_i are defined via

$$\begin{aligned} a_1 &= |A_0|^2 e^{-2b\sigma} \left((\check{R} + \gamma r^2) b^2 + 6b \frac{\check{R}}{\hat{R}} + \frac{9}{\hat{R}^2} (\check{R} - \hat{R}) - \frac{3b}{n} \right) \\ a_2 &= \frac{3b}{2n} e^{-2b\sigma} |A_0|^2 \\ a_3 &= 6W_0 A_0 e^{-b\sigma} \left(b \frac{\check{R}}{\hat{R}} + \frac{3}{\hat{R}^2} (\check{R} - \hat{R}) \right) \\ a_4 &= \gamma^{-1} e^{-2b\sigma} \left(\frac{A_0}{\mu n} \right)^2 \\ a_5 &= \frac{9}{\hat{R}^2} (\check{R} - \hat{R}) W_0^2. \end{aligned} \quad (4.5)$$

Note that due to the particular form of embedding given by Eq. (4.20), only the $(\bar{1}1)$ component of the inverse metric $k_{(w)}^{\bar{i}j}$ shows up in the F-term potential with

$$\begin{aligned} k_{(w)}^{\bar{1}1} &= \frac{3r}{2} \left(1 + \frac{|w_1|^2}{2r^3} - \frac{|w_2|^2}{r^3} \right) \\ &= \frac{3r}{16} (7 - 3 \cos \theta_1 - 3 \cos \theta_2 - \cos \theta_1 \cos \theta_2). \end{aligned} \quad (4.6)$$

The details of the stability analysis is relegated to **Appendix C**. Here we summarize the important results. Possible stable solutions are given by

$$(a) : \theta_1 = \theta_2 = 0 \quad (b) : \tilde{\psi} = 2m\pi, \theta_1 = \theta_2 = \pi \quad (4.7)$$

where $\tilde{\psi} \equiv \psi - \phi_1 - \phi_2$ and m is an integer subject to $-4\pi \leq \tilde{\psi} \leq 4\pi$.

4.1.1 Stability of case (a)

In case (a) we note that $\tilde{\psi}$ is a flat direction and the potential is independent of $\tilde{\psi}$. Also $w_1 = 0, |w_2| = 1$ which gives $F = \mathcal{F} = 1$. In order for the solution to be stable, the following approximate inequality should be met

$$16\pi^2\gamma^2\mu^2W_0^2e^{2b\sigma}r\cos^2\tilde{\psi}/2 < 1. \quad (4.8)$$

On the other hand, using the relations (2.2) and (2.4) and taking $r_\mu \lesssim R_{CY}$, one has

$$\gamma r_\mu^2 \lesssim (R_{CY}m_s)^4 \frac{m_s^4}{M_P^2} R_{CY}^2 \sim 1 \quad (4.9)$$

Using this and noting that $b\sigma \simeq 3$ as in Eq. (2.16), then Eq. (4.8) is satisfied if

$$\frac{r}{r_\mu} \cos^2\tilde{\psi} < 10^{-5}W_0^{-2}. \quad (4.10)$$

The consistency of our picture requires that $r > r_0$, where r_0 is the IR cut-off of the throat. Assuming that r_μ is comparable to the AdS scale of the throat, R , then in order for Eq. (4.10) to be satisfied we need that, h_0 , the warp factor at the tip of the throat, to be as small as $10^{-5}W_0^{-2}$. Otherwise, one has to tune $\cos\tilde{\psi}/2$ sufficiently close to 0.

Having stabilized the angular directions, we can now look at the behavior of the potential as a function of r . Because $F = \mathcal{F} = 1$, as in [6], we see that the contribution of the mobile D3-brane to the superpotential vanishes and $A = A_0$. This is subsequently labeled as “delta-flat” solution in [14]. Here “delta” represents the change into V_F due to contribution from D3-brane into superpotential.

One may ask whether or not a period of slow-roll inflation is supported while the brane is moving towards the tip. With $\mathcal{F} = 1$, we obtain

$$V_F = \frac{1}{3R\hat{R}}(a_1 + 2a_2 + a_3 + a_5) \simeq V_0 \left[1 + \frac{\gamma}{\sigma} r^2 \left(1 + \frac{5a_5}{4(a_1 + a_3 + a_5)} \right) \right] \quad (4.11)$$

where V_0 represents the value of potential in the absence of D3-brane, corresponding to setting $r = 0$. To calculate the slow-roll parameter η , first we find the normalized field, ϕ , given by

$$\phi = \sqrt{\frac{3\gamma}{\sigma}} r \quad (4.12)$$

where the brane kinetic energy has the standard form $-\partial_\mu\phi\partial^\mu\phi/2$. Calculating η one obtains that

$$\eta = \frac{\sigma}{3\gamma} \left| \frac{V,rr}{V} \right| \simeq \frac{2}{3} + \frac{5a_5}{6(a_1 + a_3 + a_5)}. \quad (4.13)$$

Interestingly enough, the first term containing the factor of $2/3$ is similar to the result of [4]. The second term containing a_5 is due to ξ corrections to the Kähler potential where the no-scale property of the four-dimensional susy is broken. On the other hand, $a_5 > 0$ and

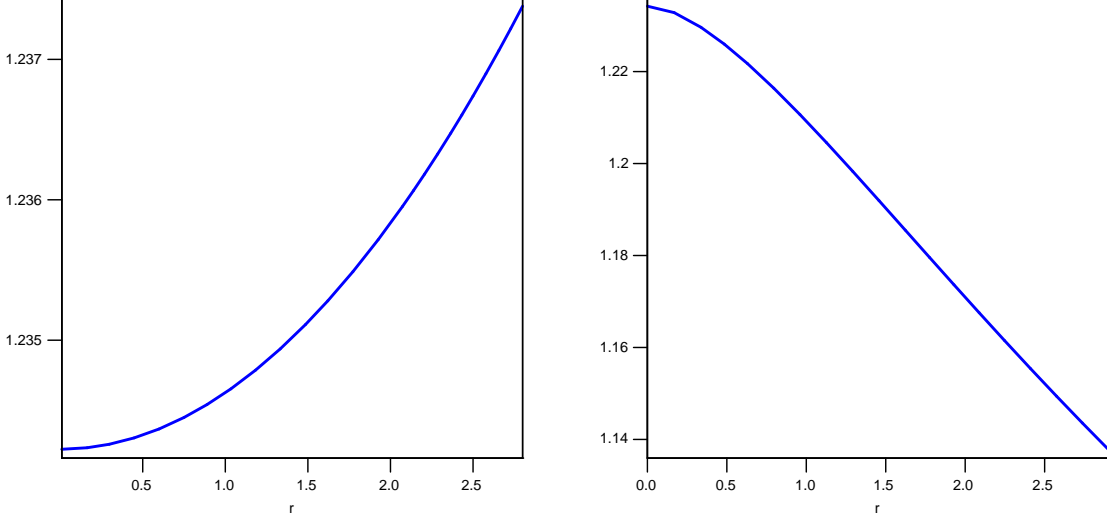


Figure 2: In this figure, V_F (in units of 10^{-8}) is plotted as a function of r for $A_0 = 1, W_0 = -8, n = 314$ with $\xi = 300, \gamma = 10^{-3}$ and $r_\mu = 2.9$ in Ouyang embedding. The left figure is for case (a) where the D3-brane is attracted towards the tip while the right figure is for case (b) where the D3-brane is attracted towards the stack of D7-branes.

$a_1 + a_3 + a_5 \sim -a_2$ with $a_2 \ll a_5$ in our background. This indicates that $\eta > 1$ and it is not possible to obtain slow-roll inflation in this embedding without fine-tuning.

The figure on the left hand side of **Fig. (2)** represents V_F for case (a). We see that as in [6], the D3-brane is attracted towards the tip of the throat. This is also easily seen from Eq. (4.11).

4.1.2 Stability of case (b)

In order for case (b) to be a stable solution, we require that $\cos \tilde{\psi}/2 = -1$ and $\tilde{\psi} = 2\pi$. This corresponds to $w_1 = -r^{3/2}$. Furthermore, the position of the D3-brane should satisfy the condition $r_c < r < r_\mu$ where r_c is approximately given by

$$r_c \simeq (8\pi\gamma\mu W_0 e^{b\sigma})^{-2}. \quad (4.14)$$

For, $r_0 \leq r \leq r_c$ the solution is unstable.

In this example we see that the contribution of D3-brane to the superpotential does not vanish, corresponding to $F = 1 + (r/r_\mu)^{3/2}$, so we find a specific “non-delta flat” solution in Ouyang embedding. In the work of [6] this solution was not a stable solution. However, in our case here, the stability of the solution is due to the additional term containing a_3 . With $|W_0| \sim 1$, the term containing a_3 dominates over other terms and plays the key role in making case (b) to be a stable solution.

To calculate η , we note that

$$V_F \simeq \frac{1}{3R\hat{R}} \left(a_1 + a_3 \mathcal{F}^{1/2n} + a_5 \right). \quad (4.15)$$

Calculating η one obtains

$$\begin{aligned}\eta &\simeq \frac{2}{3} + \frac{5a_5}{6(a_1 + a_3 + a_5)} + \frac{\sigma a_3}{4n\gamma\mu r^{1/2}F^2(a_1 + a_3 + a_5)} \left(1 - \frac{2r^{3/2}}{\mu}\right) \\ &\simeq \frac{\sigma a_3}{4n\gamma\mu r^{1/2}F^2(a_1 + a_3 + a_5)} \left(1 - \frac{2r^{3/2}}{\mu}\right).\end{aligned}\tag{4.16}$$

Looking at the behavior of η , one observes that the potential has an inflection point at r_{in} given approximately by

$$r_{in} \simeq 2^{-2/3}r_\mu\tag{4.17}$$

where $\eta = 0$. However, the potential does not stay nearly flat near the inflection point. As in case (a), the potential is too steep to allow inflation.

One also is interested in the shape of potential and whether or not the D3-brane is moving towards the tip or not. In **Fig(2)** we have plotted the potential as a function of r where σ is stabilized to its background value. We see that the D3-brane is attracted towards the D7-brane. This can also be understood analytically. The minimum, r_{min} , of the potential (4.15) is determined by

$$\begin{aligned}\left(\frac{r_{min}}{r_\mu}\right)^{1/2} \left(1 + \left(\frac{r_{min}}{r_\mu}\right)^{3/2}\right) &\simeq \frac{3\sigma}{2n\gamma r_\mu^2} \frac{-a_3}{a_3 + \frac{9}{4}a_5} \\ &\simeq \frac{1}{\gamma r_\mu^2} \gtrsim 1.\end{aligned}\tag{4.18}$$

To go to the second line, we used the approximate relation $b\sigma \sim 3$, equivalent to $\sigma \sim 3n/2\pi$, which holds in our background. The final expression is also a consequence of Eq. (4.9). In conclusion

$$\frac{r_{min}}{r_\mu} \gtrsim 1.\tag{4.19}$$

This indicates that the minimum of the D3-position is typically outside of the throat. The D3-brane is moving from the IR region into the UV region and get dissolved into D7-branes. This may provide an explicit construction of models of IR brane inflation[26] where the D3-brane leaves the IR region towards the UV region of the throat. However, one may tune the background parameters such as n and W_0 such that r_{min} is close to the the position of the D7-brane but inside the throat. In this case the D3-brane is confined between the tip of the throat and the D7-branes.

4.2 Kuperstein Embedding

The Kuperstein embedding is define by

$$F = F(z_1) = 1 - \frac{z_1}{\mu}.\tag{4.20}$$

The F-term potential is formally the same as in the Ouyang embedding, with the replacement of $w_1 \rightarrow z_1$ and $k_{(w)}^{\bar{1}1} \rightarrow k_{(z)}^{\bar{1}1}$ where

$$k_{(z)}^{\bar{1}1} = \frac{3r}{2} \left(1 - \frac{|z_1|^2}{2r^3} \right). \quad (4.21)$$

The stable solutions are

$$\begin{aligned} (a) : \quad & \theta_1 = \theta_2 = 0, \quad \varphi + \tilde{\phi} = 2n\pi \\ (b) : \quad & \theta_1 = \theta_2 = \pi, \quad \varphi - \tilde{\phi} = 2n\pi \\ (c) : \quad & \theta_1 = \theta_2, \quad \varphi = (2n+1)\pi, \quad \tilde{\phi} = (2m+1)\pi \end{aligned} \quad (4.22)$$

where m and n are integers and $\tilde{\phi} \equiv \phi_1 + \phi_2$.

In **Appendix C** we show that only solutions that lead to $z_1 = -\frac{r^{3/2}}{\sqrt{2}}$ are stable [14]. This requires that n to be odd(even) in case (a)((b)), while $m+n$ to be even in case (c).

For all three cases, we note that $F = 1 + r^{3/2}/\sqrt{2}r_\mu^{3/2}$ and V_F is formally given as in Eq. (4.15). To calculate η , we borrow Eq. (4.16) with the replacement $\mu \rightarrow \sqrt{2}\mu$ which gives

$$\eta \simeq \frac{\sigma a_3}{4n\sqrt{2}\gamma\mu r^{1/2}F^2(a_1 + a_3 + a_5)} \left(1 - \frac{\sqrt{2}r^{3/2}}{\mu} \right). \quad (4.23)$$

As before, for parameters of physical interest, this gives too big a value of η to allow for slow-roll inflation. Furthermore, there is inflection point at

$$r_{in} \simeq 2^{-1/3}r_\mu,$$

but the potential does not stay flat enough around the inflection point to allow slow-roll inflation as is clear from the large value of η given above.

The shape of the potential is similar to case (b) of the Ouyang embedding; the D3-brane is attracted towards the D7-brane if $r_{min} > r_\mu$. However, as before, one can also arrange such that $r_{min} \lesssim r_\mu$ and the D3-brane is confined between the tip of the throat and the D7-branes.

5. Conclusion and Discussions

In this work the dynamics of D3-D7 branes in an inflationary throat was studied. In the limit where W_0 is large and α' corrections to Kähler potential are included, it is shown that the dS uplifting and the moduli stabilization can be achieved without the addition of anti-D3 branes. This has the advantage that the SUSY is not broken explicitly.

We have treated ξ , the parameter corresponding to α' correction, as a constant. In a more realistic treatment, the α' correction is a function of the dilaton field. We work in a background where the dilaton is fixed. However, in calculating the covariant derivatives of W and K , one should consider dilaton as an independent field and only at the end impose the condition that dilaton is constant. This brings corrections of order ξ^2 into our background

potential Eq. (2.14). Consequently, this will change the numerics of the uplifting slightly without changing the whole picture. Furthermore, this also does not affect our conclusion in section 4 about the stability analysis of different embeddings studied. The reason is that the terms containing ξ are only important in a_5 and our discussions rely on the leading term in a_5 which is linear in ξ . Therefore, in order to keep the analysis transparent and tractable, we have neglected the effects of dilaton in ξ .

In this work, we have considered the leading α' correction to Kähler potential. We work in the large volume limit where the higher order α' corrections, which are unknown, may be neglected. It would be interesting to see how higher order corrections to Kähler potential may affect the uplifting mechanism. However, it is expected that our stability analysis remain unchanged, since our analysis there rely on the linear term in ξ as explained above.

We have looked into the shape of the inflationary potential for the radial position of the D3-brane once all angular directions are integrated out. The analysis were specifically performed for Ouyang and Kuperstein embeddings which define two characteristic classes of embeddings for the wrapped D7-branes. In Kuperstein embedding the D3-brane is attracted towards the stack of D7-branes while for Ouyang embedding it can move towards the tip of the throat or towards the D7-branes, depending on the stabilized angular directions. We have seen that the potential in both cases is too steep to allow a period of slow-roll inflation. This has origin in largeness of $|W_0|$ which is required in our uplifting mechanism. Unlike [14], the contributions to the potential from nonperturbative corrections to the superpotential can not be made large enough to cancel out the contributions from W_0 . It is expected that this conclusion to be generic, holding for other embeddings too. It would be interesting to perform a systematic investigation for other embeddings to see whether or not this expectation still holds.

Acknowledgments

We thank Cliff Burgess, Jim Cline and Keshav Dasgupta for their initial contributions and for many discussions and comments. We Also thank X. Chen for discussions. H.F. thanks Banff International Research Station (BIRS) for hospitality when this work was initiated.

A. Uplifting by α' correction

Here we study uplifting and Kähler modulus stabilization in more details. The potential, up to second order in ξ , is given by Eq. (2.16)

$$V_F \simeq \frac{bW_0}{2\sigma^2} e^{-b\sigma} + \frac{3W_0^2\xi}{2^{11/2}\sigma^{9/2}} - \frac{9W_0^2\xi^2}{256\sigma^6}.$$

As mentioned, we have neglected terms containing $e^{-2b\sigma}$, which is a good approximation for large enough W_0 . The minimum of Eq. (2.16) is given by

$$|W_0|\xi b^{3/2} = \frac{2^{11/2} x^{5/2} (x+2) e^{-x}}{27 (1 - 2^{-1/2} \xi b^{3/2} x^{-3/2})} \equiv f(x) \quad (\text{A.1})$$

where we have defined $b\sigma = x$. Furthermore, requiring that the potential is positive at the minimum, implies that

$$|W_0|\xi b^{3/2} > \frac{2^{9/2} e^{-x} x^{5/2}}{3 \left(1 - \frac{3}{2^{5/2}} \xi b^{3/2} x^{-3/2}\right)} \equiv g(x) \quad (\text{A.2})$$

With some efforts, one can check that the functions f and g have maximum at x_f and x_g , respectively, given by

$$x_f \simeq 3.1 - 3.2 \hat{\xi} \quad , \quad x_g \simeq 2.5 - 2.3 \hat{\xi} \quad (\text{A.3})$$

Looking at the plots of f and g , one concludes that in order to satisfy conditions (A.1) and (A.2), one requires that $x_g \leq x \leq x_f$ and $f(x_g) \leq |W_0|^2 \xi b^{3/2} \leq f(x_f)$, or

$$2.5 - 2.3 \hat{\xi} \leq b\sigma \leq 3.1 - 3.2 \hat{\xi} \quad , \quad 6.1 + 9.2 \hat{\xi} \leq |W_0|^2 \xi b^{3/2} \leq 6.5 + 13 \hat{\xi}. \quad (\text{A.4})$$

This leads to the following useful relations

$$b\sigma \simeq 3 \quad , \quad |W_0|\xi b^{3/2} \simeq 6.5. \quad (\text{A.5})$$

We have checked many numerical examples where the relations in Eq. (A.5) are hold with reasonable accuracies.

B. The Conifold

Here we briefly summarized the representation of conifold in w and z coordinates. The conifold is defined by

$$\sum_{m=1}^4 z_m^2 = 0 \quad (\text{B.1})$$

with the Kähler potential

$$k = \left(\sum_{m=1}^4 |z_m|^2 \right)^{2/3} = r^2. \quad (\text{B.2})$$

The conifold in z -coordinate is given by

$$\begin{aligned}
z_1 &= \frac{r^{3/2}}{\sqrt{2}} e^{i\psi/2} \left[\cos\left(\frac{\theta_1 + \theta_2}{2}\right) \cos\left(\frac{\phi_1 + \phi_2}{2}\right) + i \cos\left(\frac{\theta_1 - \theta_2}{2}\right) \sin\left(\frac{\phi_1 + \phi_2}{2}\right) \right] \\
z_2 &= \frac{r^{3/2}}{\sqrt{2}} e^{i\psi/2} \left[-\cos\left(\frac{\theta_1 + \theta_2}{2}\right) \sin\left(\frac{\phi_1 + \phi_2}{2}\right) + i \cos\left(\frac{\theta_1 - \theta_2}{2}\right) \cos\left(\frac{\phi_1 + \phi_2}{2}\right) \right] \\
z_3 &= \frac{r^{3/2}}{\sqrt{2}} e^{i\psi/2} \left[-\sin\left(\frac{\theta_1 + \theta_2}{2}\right) \cos\left(\frac{\phi_1 - \phi_2}{2}\right) + i \sin\left(\frac{\theta_1 - \theta_2}{2}\right) \sin\left(\frac{\phi_1 - \phi_2}{2}\right) \right] \\
z_4 &= \frac{r^{3/2}}{\sqrt{2}} e^{i\psi/2} \left[-\sin\left(\frac{\theta_1 + \theta_2}{2}\right) \sin\left(\frac{\phi_1 - \phi_2}{2}\right) - i \sin\left(\frac{\theta_1 - \theta_2}{2}\right) \cos\left(\frac{\phi_1 - \phi_2}{2}\right) \right]. \tag{B.3}
\end{aligned}$$

Notice that r denotes proper distance up the throat, and $r = 0$ corresponds to the throat's tip, which is singular if the conifold is not deformed.

Upon linear transformations (3.11) one goes to the w -coordinate where now the conifold is given by

$$\begin{aligned}
w_1 &= r^{3/2} e^{\frac{i}{2}(\psi - \phi_1 - \phi_2)} \sin\frac{\theta_1}{2} \sin\frac{\theta_2}{2} \\
w_2 &= r^{3/2} e^{\frac{i}{2}(\psi + \phi_1 + \phi_2)} \cos\frac{\theta_1}{2} \cos\frac{\theta_2}{2} \\
w_3 &= r^{3/2} e^{\frac{i}{2}(\psi + \phi_1 - \phi_2)} \cos\frac{\theta_1}{2} \sin\frac{\theta_2}{2} \\
w_4 &= r^{3/2} e^{\frac{i}{2}(\psi - \phi_1 + \phi_2)} \sin\frac{\theta_1}{2} \cos\frac{\theta_2}{2}. \tag{B.4}
\end{aligned}$$

C. The stability analysis

Here we study in more details the angular stability of different solutions for both Ouyang and Kuperstein embeddings

C.1 Ouyang embedding

The independent angular variables are $\{\Psi_i\} = \{\theta_1, \theta_2, \tilde{\psi}\}$, where $\tilde{\psi} \equiv \psi - \phi_1 - \phi_2$. Furthermore, we note that V_F as given in Eq. (4.3) is a function of $|w_1|^2, |w_2|^2$ and $w_1 + \bar{w}_1$. Define $x_1 = |w_1|^2, x_2 = |w_2|^2$ and $x_3 = w_1 + \bar{w}_1$. As argued in [14], finding the stable values of Ψ_i independent of r requires that

$$\frac{\partial x_i}{\partial \Psi_j} = 0 \tag{C.1}$$

The sets of solutions to above equations are

$$\begin{aligned}
(a) : \theta_1 = \theta_2 = 0 & & (b) : \tilde{\psi} = 2m\pi, \theta_1 = \theta_2 = \pi \\
(c) : \tilde{\psi} = (2m+1)\pi, \theta_1 = 0, \theta_2 = \pi & & (d) : \tilde{\psi} = (2m+1)\pi, \theta_1 = \pi, \theta_2 = 0, \tag{C.2}
\end{aligned}$$

where m is an integer subject to $-4\pi \leq \tilde{\psi} \leq 4\pi$.

Below we demonstrate that only cases (a) and (b) could be stable. Define $X_i = \partial V / \partial x_i$. Then at the extrema given by Eq. (C.1) the mass matrix, V_{ij} , is given by

$$V_{ij} = \frac{\partial^2 V}{\partial \Psi_i \partial \Psi_j} = X_k \frac{\partial^2 x_k}{\partial \Psi_i \partial \Psi_j}. \quad (\text{C.3})$$

The nonzero components of the mass matrix are:

$$\begin{aligned} (\text{a}) \quad & V_{\theta_1 \theta_1} = V_{\theta_2 \theta_2} = -\frac{r^3}{2} X_2 \quad , \quad V_{\theta_1 \theta_2} = \frac{r^{3/2}}{2} X_3 \cos \frac{\tilde{\psi}}{2} \\ (\text{b}) \quad & V_{\theta_1 \theta_1} = V_{\theta_2 \theta_2} = -\frac{r^3}{2} X_1 - \frac{r^{3/2}}{2} \cos \frac{\tilde{\psi}}{2} X_3 \quad , \quad V_{\tilde{\psi} \tilde{\psi}} = -\frac{r^{3/2}}{2} \cos \frac{\tilde{\psi}}{2} X_3 \\ (\text{c}) \quad & V_{\theta_1 \theta_1} = \frac{r^3}{2} X_1 \quad , \quad V_{\theta_2 \theta_2} = \frac{r^3}{2} X_2 \quad , \quad V_{\theta_1 \tilde{\psi}} = -\frac{r^{3/2}}{2} \sin \frac{\tilde{\psi}}{2} X_3 \\ (\text{d}) \quad & V_{\theta_1 \theta_1} = \frac{r^3}{2} X_2 \quad , \quad V_{\theta_2 \theta_2} = \frac{r^3}{2} X_1 \quad , \quad V_{\theta_2 \tilde{\psi}} = -\frac{r^{3/2}}{2} \sin \frac{\tilde{\psi}}{2} X_3 \end{aligned} \quad (\text{C.4})$$

In the cases of (c) and (d) one can check that there is a negative eigenvalue, so these cases are unstable, corresponding to $w_1 = w_2 = 0$. The stability of the other two solutions depends on the sign of X_i given by

$$\begin{aligned} X_2 &= -\frac{a_4 \mathcal{F}_n^{\frac{1}{n}-1}}{2r^2 R \hat{R}} \\ X_1 &= \frac{\mathcal{F}_n^{\frac{1}{n}-1}}{3\mu^2 R \hat{R}} \left[\frac{a_1}{n} - a_2 \left(1 - \frac{1}{n}\right) \left(2 - \frac{w_1 + \bar{w}_1}{\mu}\right) \mathcal{F}^{-1} + \frac{a_3}{2n} \mathcal{F}^{\frac{-1}{2n}} + \frac{3\mu^2}{4r^2} a_4 - a_4 \left(1 - \frac{1}{n}\right) k_w^{\bar{1}1} \mathcal{F}^{-1} \right] \\ X_3 &= \frac{-\mathcal{F}_n^{\frac{1}{n}-1}}{3\mu R \hat{R}} \left[\frac{a_1}{n} + a_2 - a_2 \left(1 - \frac{1}{n}\right) \left(2 - \frac{w_1 + \bar{w}_1}{\mu}\right) \mathcal{F}^{-1} + \frac{a_3}{2n} \mathcal{F}^{\frac{-1}{2n}} - a_4 \left(1 - \frac{1}{n}\right) k_w^{\bar{1}1} \mathcal{F}^{-1} \right] \end{aligned} \quad (\text{C.5})$$

From the form of a_i given in Eq. (4.5) we note that all a_i except a_3 are positive. This implies that $X_2 < 0$. Furthermore, $|a_3|/n > a_1/n > a_2$ which will be useful later.

C.1.1 Stability of case (a)

For case (a) we note that $\tilde{\psi}$ is a flat direction and the potential is independent of $\tilde{\psi}$. In order for solution to be stable we require that $X_2 < 0$ and $r^3 X_2^2 - X_3^2 \cos^2 \tilde{\psi}/2 > 0$. As mentioned above, the first condition is always satisfied. On the other hand, we have $w_1 = 0, |w_2| = 1$ which gives $k_w^{\bar{1}1} = 0$ and $\mathcal{F} = 1$. Calculating X_3 , we find

$$X_3 = \frac{-1}{3\mu R \hat{R}} \left(\frac{a_1}{n} + \left(\frac{2}{n} - 1\right) a_2 + \frac{a_3}{2n} \right) \simeq \frac{-a_3}{6n \mu R \hat{R}}. \quad (\text{C.6})$$

The stability of the solution is therefore approximately translated into

$$16\pi^2 \gamma^2 \mu^2 W_0^2 e^{2b\sigma} r \cos^2 \tilde{\psi}/2 < 1. \quad (\text{C.7})$$

C.1.2 Stability of case (b)

For the stability of case (b) we require that $X_3 \cos \tilde{\psi}/2 < 0$ and $X_3 \cos \tilde{\psi}/2 + r^{3/2}X_1 < 0$. Furthermore

$$X_3 \sim -\frac{\mathcal{F}^{-1+\frac{1}{n}} a_3}{3\mu R \hat{R}} > 0. \quad (\text{C.8})$$

Demanding that $X_3 \cos \tilde{\psi}/2 < 0$ requires that $\cos \tilde{\psi}/2 = -1$ and $\tilde{\psi} = 2\pi$. This corresponds to $w_1 = -r^{3/2}$.

On the other hand, one can also check that

$$X_3 \cos \tilde{\psi}/2 + r^{3/2}X_1 \sim \frac{\mathcal{F}^{-1+\frac{1}{n}}}{3\mu^2 R \hat{R}} \left[\frac{a_3}{2n} \mu \mathcal{F}^{-1/2n} \left(1 + \frac{r^{3/2}}{r_\mu^{3/2}}\right) + \frac{3\mu^2}{4r^{1/2}} a_4 \right]. \quad (\text{C.9})$$

Since $a_3 < 0$, the above expression changes sign for sufficiently small r . In conclusion, we see that case (b) with $\tilde{\psi} = 2\pi$ is stable for the range $r_c < r < r_\mu$, while unstable for $r_0 < r < r_c$, where r_c is approximately given by the root of the term in the bracket (C.9) as

$$r_c \simeq (8\pi\gamma\mu W_0 e^{b\sigma})^{-2}. \quad (\text{C.10})$$

C.2 Kuperstein Embedding

Here we find the stable position of the angular variables $\{\Psi_i\} = \{\theta_1, \theta_2, \psi, \tilde{\phi}\}$, where $\tilde{\phi} \equiv \phi_1 + \phi_2$. The potential V_F is now a function of $z_1 + \bar{z}_1$ and $|z_1|^2$. As in Ouyang embedding, the stable values of Ψ_i satisfy:

$$\frac{\partial(z_1 + \bar{z}_1)}{\partial\Psi_j} = 0, \quad \frac{\partial|z_1|^2}{\partial\Psi_j} = 0 \quad (\text{C.11})$$

The solutions are

$$\begin{aligned} (a) : & \theta_1 = \theta_2 = 0, \varphi + \tilde{\phi} = 2n\pi \\ (b) : & \theta_1 = \theta_2 = \pi, \varphi - \tilde{\phi} = 2n\pi \\ (c) : & \theta_1 = \theta_2, \varphi = (2n+1)\pi, \tilde{\phi} = (2m+1)\pi \\ (d) : & \theta_{1(2)} = 0, \theta_{2(1)} = \pi, \varphi = (2n+1)\pi, \tilde{\phi} = 2m\pi \\ (e) : & \theta_{1(2)} = 0, \theta_{2(1)} = \pi, \varphi = 2n\pi, \tilde{\phi} = (2m+1)\pi \end{aligned} \quad (\text{C.12})$$

where m and n are integers.

Below we show that only solutions that lead to $z_1 = -\frac{r^{3/2}}{\sqrt{2}}$ are stable [14]. The mass matrix is given by

$$V_{ij} = \frac{\partial V}{\partial\Psi_i \partial\Psi_j} = Y_1 \frac{\partial^2(z_1 + \bar{z}_1)}{\partial\Psi_i \partial\Psi_j} + Y_2 \frac{\partial^2|z_1|^2}{\partial\Psi_i \partial\Psi_j} \quad (\text{C.13})$$

where

$$Y_1 \equiv \frac{\partial V_F}{\partial(z_1 + \bar{z}_1)} \quad , \quad Y_2 \equiv \frac{\partial V_F}{\partial|z_1|^2} \quad (\text{C.14})$$

given by

$$\begin{aligned} Y_1 &= -\frac{\mathcal{F}_n^{\frac{1}{n}-1}}{3\mu R\hat{R}} \left[\frac{a_1}{n} + a_2 - a_2\left(1 - \frac{1}{n}\right)\left(2 - \frac{z_1 + \bar{z}_1}{\mu}\right)\mathcal{F}^{-1} + \frac{a_3}{2n}\mathcal{F}^{\frac{-1}{2n}} - a_4\left(1 - \frac{1}{n}\right)k_z^{\bar{1}1}\mathcal{F}^{-1} \right] \\ Y_2 &= \frac{\mathcal{F}_n^{\frac{1}{n}-1}}{3\mu^2 R\hat{R}} \left[\frac{a_1}{n} - a_2\left(1 - \frac{1}{n}\right)\left(2 - \frac{z_1 + \bar{z}_1}{\mu}\right)\mathcal{F}^{-1} + \frac{a_3}{2n}\mathcal{F}^{\frac{-1}{2n}} - a_4\left(1 - \frac{1}{n}\right)k_z^{\bar{1}1}\mathcal{F}^{-1} - a_4\frac{3\mu^2}{4r^2} \right]. \end{aligned} \quad (\text{C.15})$$

We see that Y_1 is formally the same as X_1 with the replacement of $w \rightarrow z$, while Y_2 is similar to X_1 except with a change of sign in the term containing $\mu^2 a_4$. Since $|a_3|/n > a_1/n > a_2$ and $a_3 < 0$, Y_1 is always positive while Y_2 is always negative.

The nonzero components of the mass matrix are given by

$$\begin{aligned} (a) \quad & V_{\theta_1\theta_1} = V_{\theta_2\theta_2} = -(-1)^n \frac{\sqrt{2}r^{3/2}}{4} Y_1 - \frac{r^3}{4} Y_2, \quad V_{\theta_1\theta_2} = \cos\psi V_{\theta_1\theta_1} \\ & V_{\psi\psi} = V_{\tilde{\phi}\tilde{\phi}} = V_{\psi\tilde{\phi}} = -(-1)^n \frac{\sqrt{2}r^{3/2}}{4} Y_1. \\ (b) \quad & V_{\theta_1\theta_1} = V_{\theta_2\theta_2} = (-1)^n \frac{\sqrt{2}r^{3/2}}{4} Y_1 - \frac{r^3}{4} Y_2, \quad V_{\theta_1\theta_2} = \cos\psi V_{\theta_1\theta_1} \\ & V_{\psi\psi} = V_{\tilde{\phi}\tilde{\phi}} = V_{\psi\tilde{\phi}} = (-1)^n \frac{\sqrt{2}r^{3/2}}{4} Y_1. \\ (c) \quad & V_{\theta_1\theta_1} = V_{\theta_2\theta_2} = -V_{\theta_1\theta_2} = (-1)^{m+n} \frac{\sqrt{2}r^{3/2}}{4} Y_1 - \frac{r^3}{4} Y_2, \\ & V_{\psi\psi} = (-1)^{m+n} \frac{\sqrt{2}r^{3/2}}{4} Y_1, \quad V_{\psi\tilde{\phi}} = \cos\theta_1 V_{\psi\psi} \\ & V_{\tilde{\phi}\tilde{\phi}} = (-1)^{m+n} \frac{\sqrt{2}r^{3/2}}{4} Y_1 - \frac{r^3}{4} Y_2 \sin^2\theta_1 \\ (d) \quad & V_{\theta_1\theta_1} = V_{\theta_2\theta_2} = V_{\theta_1\theta_2} = \frac{r^3}{4} Y_2, \\ & V_{\theta_1\tilde{\psi}} = V_{\theta_1\tilde{\phi}} = V_{\theta_2\tilde{\psi}} = V_{\theta_2\tilde{\phi}} = \frac{(-1)^{n+m}\sqrt{2}}{4} r^{3/2} Y_1. \\ (e) \quad & V_{\theta_1\theta_1} = V_{\theta_2\theta_2} = -V_{\theta_1\theta_2} = \frac{r^3}{4} Y_2, \\ & V_{\theta_1\tilde{\psi}} = V_{\theta_1\tilde{\phi}} = -V_{\theta_2\tilde{\psi}} = V_{\theta_2\tilde{\phi}} = \frac{(-1)^{n+m}\sqrt{2}}{4} r^{3/2} Y_1. \end{aligned} \quad (\text{C.16})$$

Looking at the eigenvalues of the mass matrix, one easily finds that case (d) and (e) are unstable. More explicitly, one encounters the eigenvalues

$$\frac{r}{4} \left(r^2 Y_2 \pm (-1)^m \sqrt{r^4 Y_2^2 + 4r Y_1^2} \right)$$

which indicates the existence of instability.

The nonzero eigenvalues of case (a) are

$$\lambda_1^a = -\frac{(-1)^n \sqrt{2}}{2} r^{3/2} Y_1 \quad , \quad \lambda_{2,3}^a = -\frac{1}{4} \left((-1)^n \sqrt{2} r^{3/2} Y_1 + Y_2 r^3 \right) (1 \pm \cos \psi) \quad (\text{C.17})$$

Since $Y_1 > 0$ and $Y_2 < 0$, to get a stable solution we requires n to be odd. This corresponds to $z_1 = -\frac{r^{3/2}}{\sqrt{2}}$ as in [14].

The nonzero eigenvalues of case (b) are the same as in case (a) with an overall minus sign. So we see that for this case to be stable, we need n to be even corresponding to $z_1 = -\frac{r^{3/2}}{\sqrt{2}}$. This indicates that F and $k_w^{\bar{1}1}$ are the same as in case (a) so the potential is exactly the same as in case (a).

Finally, for case (c) to be stable we require that

$$(-1)^{m+n} \sqrt{2} r^{3/2} Y_1 - r^3 Y_2 > 0 \quad , \quad Y_1 \sin^2 \theta_1 \left(\sqrt{2} r^{3/2} Y_1 - (-1)^{m+n} r^3 Y_2 \right) > 0 \quad (\text{C.18})$$

To satisfy these conditions, we need $m + n$ to be even. This in turn implies that $z_1 = -\frac{r^{3/2}}{\sqrt{2}}$ and the potential is the same as in case (a) and (b).

References

- [1] I. R. Klebanov and M. J. Strassler, “Supergravity and a confining gauge theory: Duality cascades and chiSB-resolution of naked singularities,” *JHEP* **0008**, 052 (2000) [arXiv:hep-th/0007191].
- [2] S. B. Giddings, S. Kachru and J. Polchinski, “Hierarchies from fluxes in string compactifications,” *Phys. Rev. D* **66**, 106006 (2002) [arXiv:hep-th/0105097].
- [3] S. Kachru, R. Kallosh, A. Linde and S. P. Trivedi, “De Sitter vacua in string theory,” *Phys. Rev. D* **68**, 046005 (2003) [arXiv:hep-th/0301240].
- [4] S. Kachru, R. Kallosh, A. Linde, J. M. Maldacena, L. P. McAllister and S. P. Trivedi, “Towards inflation in string theory,” *JCAP* **0310**, 013 (2003) [arXiv:hep-th/0308055].
- [5] C. P. Burgess, R. Kallosh and F. Quevedo, “de Sitter string vacua from supersymmetric D-terms,” *JHEP* **0310**, 056 (2003) [arXiv:hep-th/0309187].
- [6] C. P. Burgess, J. M. Cline, K. Dasgupta and H. Firouzjahi, “Uplifting and inflation with D3 branes,” *JHEP* **0703**, 027 (2007) [arXiv:hep-th/0610320].
- [7] G. Dvali and S.-H.H. Tye, ”Brane Inflation”, *Phys. Lett.* **B450** (1999) 72, hep-ph/9812483.
- [8] C. P. Burgess, M. Majumdar, D. Nolte, F. Quevedo, G. Rajesh and R. J. Zhang, *JHEP* **07** (2001) 047, hep-th/0105204 ; G. R. Dvali, Q. Shafi and S. Solganik, “D-brane inflation,” hep-th/0105203.
- [9] S. H. Henry Tye, “Brane inflation: String theory viewed from the cosmos,” *Lect. Notes Phys.* **737**, 949 (2008) [arXiv:hep-th/0610221]; J. M. Cline, “String cosmology,” arXiv:hep-th/0612129; C. P. Burgess, “Lectures on Cosmic Inflation and its Potential Stringy Realizations,” *PoS P2GC*, 008 (2006) [*Class. Quant. Grav.* **24**, S795 (2007)] [arXiv:0708.2865 [hep-th]]; L. McAllister and E. Silverstein, “String Cosmology: A Review,” *Gen. Rel. Grav.* **40**, 565 (2008) [arXiv:0710.2951 [hep-th]].

- [10] H. Firouzjahi and S. H. H. Tye, “Closer towards inflation in string theory,” *Phys. Lett. B* **584**, 147 (2004) [arXiv:hep-th/0312020].
- [11] S. E. Shandera, “Slow roll in brane inflation,” *JCAP* **0504**, 011 (2005) [arXiv:hep-th/0412077].
- [12] L. McAllister, “An inflaton mass problem in string inflation from threshold corrections to volume stabilization,” *JCAP* **0602**, 010 (2006) [arXiv:hep-th/0502001].
- [13] D. Baumann, A. Dymarsky, I.R. Klebanov, J. Maldacena, L. McAllister and A. Murugan, “On D3-brane potentials in compactifications with fluxes and wrapped D-branes,” *JHEP* **0611** 031 (2006) [hep-th/0607050].
- [14] D. Baumann, A. Dymarsky, I.R. Klebanov and L. McAllister, “Towards an explicit model of D-brane inflation,” [arXiv:0706.0360 (hep-th)].
- [15] K. Becker, M. Becker, M. Haack and J. Louis, “Supersymmetry breaking and alpha'-corrections to flux induced potentials,” *JHEP* **0206**, 060 (2002) [arXiv:hep-th/0204254].
- [16] V. Balasubramanian and P. Berglund, “Stringy corrections to Kähler potentials, SUSY breaking, and the cosmological constant problem,” *JHEP* **0411**, 085 (2004) [arXiv:hep-th/0408054].
- [17] D. Cremades, M.-P. Garcia del Moral, F. Quevedo and K. Suruliz, “Moduli stabilization and de Sitter string vacua from magnetized D7 branes,” [hep-th/0701154].
- [18] A. Misra and P. Shukla, arXiv:0707.0105 [hep-th]. A. Misra and P. Shukla, *Nucl. Phys. B* **800**, 384 (2008) [arXiv:0712.1260 [hep-th]].
- [19] P. Ouyang, “Holomorphic D7-branes and flavored $N = 1$ gauge theories,” *Nucl. Phys. B* **699**, 207 (2004) [arXiv:hep-th/0311084].
- [20] S. Kuperstein, “Meson spectroscopy from holomorphic probes on the warped deformed conifold,” *JHEP* **0503**, 014 (2005) [arXiv:hep-th/0411097].
- [21] A. Krause and E. Pajer, “Chasing Brane Inflation in String-Theory,” arXiv:0705.4682 [hep-th].
- [22] E. Pajer, “Inflation at the Tip,” *JCAP* **0804**, 031 (2008) [arXiv:0802.2916 [hep-th]].
- [23] H. Y. Chen, J. O. Gong and G. Shiu, “Systematics of multi-field effects at the end of warped brane inflation,” arXiv:0807.1927 [hep-th].
- [24] K. Dasgupta, C. Herdeiro, S. Hirano and R. Kallosh, “D3/D7 inflationary model and M-theory,” *Phys. Rev. D* **65**, 126002 (2002) [arXiv:hep-th/0203019]; K. Dasgupta, J. P. Hsu, R. Kallosh, A. Linde and M. Zagermann, “D3/D7 brane inflation and semilocal strings,” *JHEP* **0408**, 030 (2004) [arXiv:hep-th/0405247].
- [25] M. Haack, R. Kallosh, A. Krause, A. Linde, D. Lust and M. Zagermann, “Update of D3/D7-Brane Inflation on $K3 \times T^2/Z_2$,” arXiv:0804.3961 [hep-th].
- [26] X. Chen, “Multi-throat brane inflation,” *Phys. Rev. D* **71**, 063506 (2005) [arXiv:hep-th/0408084]; X. Chen, “Inflation from warped space,” *JHEP* **0508**, 045 (2005) [arXiv:hep-th/0501184]; S. Thomas and J. Ward, “IR Inflation from Multiple Branes,” *Phys. Rev. D* **76**, 023509 (2007) [arXiv:hep-th/0702229]; J. E. Lidsey and I. Huston, *JCAP* **0707**, 002 (2007) [arXiv:0705.0240 [hep-th]]; R. Bean, X. Chen, H. V. Peiris and J. Xu, “Comparing Infrared Dirac-Born-Infeld Brane Inflation to Observations,” *Phys. Rev. D* **77**, 023527 (2008) [arXiv:0710.1812 [hep-th]]. B. Underwood, “Brane Inflation is Attractive,” arXiv:0802.2117 [hep-th].